Serbian Tribology Society

SERBIATRIB '25

19th International Conference on Tribology

Faculty of Engineering University of Kragujevac

Kragujevac, Serbia, 14 – 16 May 2025

Research paper DOI:10.24874/ST.25.183

IMPACT TESTS FOR TWO COMPOSITES FOR MARINE APPLICATIONS

Ioana Gabriela CHIRACU[1], Constantin GEORGESCU[2], George Cătălin CRISTEA, George Ghiocel OJOC, Mihail BOȚAN, Alexandru Viorel VASILIU, Lorena DELEANU*

[1] "Dunarea de Jos" University, Faculty of Engineering, Galati, Romania

[2] National Institute for Aero-space Research "Elie Carafoli" (INCAS), Bucharest, Romania,

[3] Autonomous Flight Technologies, Clinceni, Romania

*Corresponding author: lorena.deleanu@ugal.ro

Abstract: *This paper presents a comparison between two composites fabricated with the same quadrialxial glass fiber fabric (8 layers) and an epoxy resin (SikaBiresin® CR82 with hardener CH80-2), but one with a mat layer (Coremat Xi 3) in the middle of the composite. The influence of impact energy and material type is discussed taking into account the graphs force – time, absorbed energy – time, displacement – time and velocity – time. Several parameters extracted from these curves are pointed out (maximum force, maximum displacement, duration of the impact) for the following range of the impact energy 50-150 J. Impact velocity was measured as 4.37±0.05 m/s. Both composites exhibited only partial penetration. At low energy imapct, the behavior of these two composites is not sensitive to composite architecture, but increasing the impact energy, the composites with Coremat Xi 3 has a better behavior, and* F_{max} *was reduced with appprox. 4000 N for the composites with Coremat Xi 3 for impact energies of 100 J and with 7490 N for impact energy of 150 J. Higher absorbed energy for these composites is obtained because of the plateaux generated by the force, during a longer impactor displacement in contact with the composite. The composite without mat (Q-g) absorbes 76.84% of the impact energy of 50 J, 82,82% for impact of 100 J, and 85.74% at 150 J. The composite with mat (QM-g), absorbs 79.66% at impact of 50 J, 89.10% at 100 J and 92.42% at 150 J. Taking into account this parameter for ranking the composites, the composite with mat has a better behavior. The results obtained for these two composites recommend them for marine applications.*

Keywords: *Quadriaxial glass fiber fabric, epoxy resin, mat, impact test, hemispherical impactor, maximum force.*

1. INTRODUCTION

Fiber-reinforced composites are made of a polymer matrix reinforced with fibers, such as carbon fibers, glass fibers or polymeric fibers. These materials are very important for engineering applications because of their specific high stiffness, fatigue performance, good chemical and thermal resistance, but their price depend on fiber type, matrix quality and fabrication process [1], [2]. Due to their advantages, fiber reinforced composites are now used to replace traditional metallic materials and widely utilized in aircraft, defense industries, automotive structures, sports equipment, ground transportation and construction, but this study is focused on testing new designed glass fiber composite for marine industry [3]-[6], including military applications [7]. In order to use them in the particular marine structural design, it becomes extremely important to understand their mechanical behavior under particular loading determined by the application [8], including impact [9], [10].

Composites with glass fibers and epoxy resin matrix have significantly higher impact strength and durability than monolithic materials, but their behavior under impact depends on several factors, such as the geometry and orientation of the fibers, their density and distribution, and the impact velocity and energy.

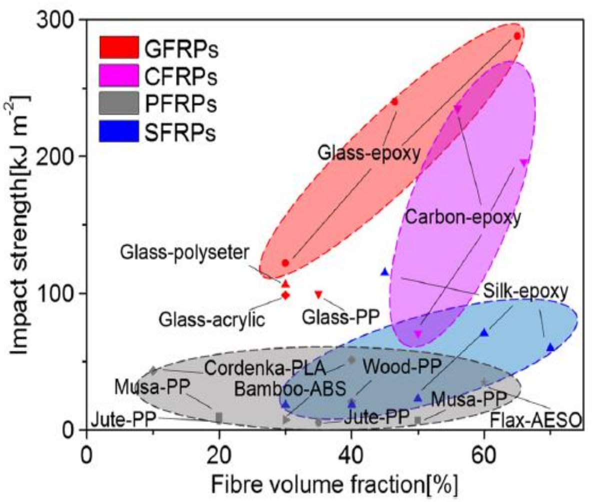

Figure 1. Impact strength of polymer composites reinforced with fibres; GFRP – glass fiber einforced plastics, CFRP – carbon fibre Reinforced plastics, PFRP – plant fibre reinforced plastics and SFRP – silk fibre reinforced plastics [11]

From Figure 1, one may notice that the "competition" for a better impact resistance is developing between glass fiber composites and carbon fiber composites, both groups with epoxy matrix.

A relevant review, written by Moritz A.P. et al. [12], almost 25 years ago, presented the applications of fiber reinforced composites for ship structure, even for defence applications. Other reviews on this subject presents new ships designs, using composites [13], [14],

For marine applications, characterization of composites by tensile, bending tests is not enough to design these structures [15], [16]. And thus, impact tests have become relevant for composite structures [17]-[19].

The objective of this study is to differentiate the impact behavior of two designed composites, for marine applications, in order to establish the influence of introducing one layer of mat in the composite architecture and the influence of impact energy.

2. MATERIALS, COMPOSITES FABRICATION AND TEST METHODOLOGY

2.1 Materials and Fabrication

Two composites were designed, both with quadriaxial glass fiber fabric and epoxy resin, one having a mat layer in the middle.

The fabric is organised in four sublayers, with orientation (0°/+45°/90°/-45°) (Table 1), which assumes from the outset that the fabric will have a quasi-isotropic behavior. The trade name is WTVQX1200-1 E-glass, Q1200E10Q, supplied by Castro Composites (Porriño, Pontevedra, España) [20].

Even from the beginning of this millenium, Sutherland L.S et al. [21] underlined that the testing of unidirectional fiber composites has been delivering important information for introducing these composites in marine structure designs.

Table 1. Characteristics of quadriaxial fabric [20]

Sublayer	Layer Orientation	Fiber Type [Tex]	Area Density [g/m^2]
1.	0 °C	600	283
2.	45 °C	300 + 600	300
3.	90 °C	600	307
4.	−45 °C	300 + 600	300
Auxilliary yarn		76 DTex	10
			Total: 1200 g/m^2 (±%3)

The measured diameters of glass fibers are in the range 11.36 μm and 17.05 μm. Figure 2 presents the elemental composition of glass fibers, differentiated for core and jacket, from an EDX analysis, as also reported in [22]. The glass fiber type is close to S class, but the higher concentration in Boron (B) favors a better response to impact.

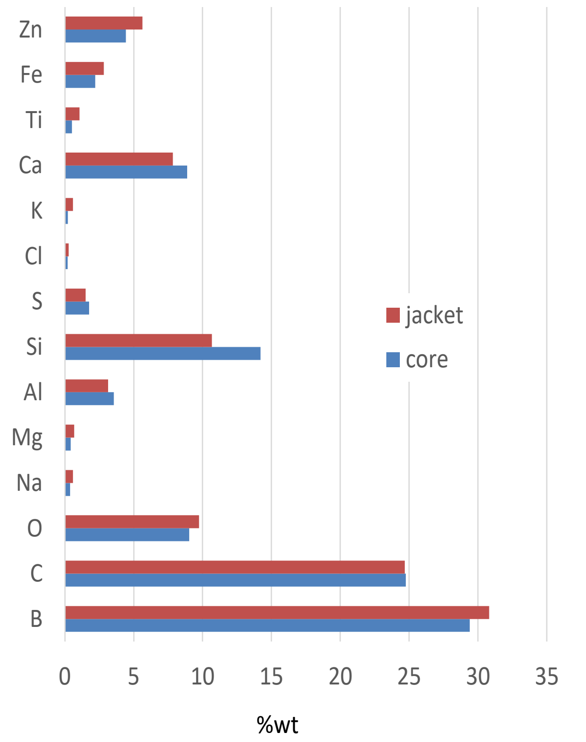

Figure 2. Elemental glass fiber composition (EDX)

After an up-to-date documentation in the field of resins for fiberglass composites [23], [24], [25] we selected Biresin® CR82 two-component resin with CH80-2 hardener from the range offered by the manufacturer Sika Group [26].

There are several characteristics of the epoxy resin. The massic mixing ratio for resin SikaBiresin® CR82 and hardener Biresin® CH80-2 is 100/27, the pot life (100g/RT) is approx. 80 minutes. The resulted epoxy resin has the following mechanical characteristics: 90 MPa for tensile strength, 3 GPa for Young modulus, 5.6% for strain at break, 130 MPa for flexural strength, 3.2 GPa for flexural modulus and 1.14 kg/m^3 for density [26].

The mat is produced by Lantor, Veenendaal, The Netherlands and supplied by Rompolimer SA (Bucharest, Romania). Whether present in the construction of ships, automotive parts, leisure and sport equipment or industrial components, Coremat® Xi3 offers an acceptable designing compromise between strength, flexibility and aesthetics, being used as a base material and/or a barrier against fiberglass imprinting on the surface of final composite products.

Coremat® Xi3 is made from a non-woven polyester with integrated microspheres, which helps to improve mechanical properties of composites and it is compatible with a wide range of resins, including unsaturated polyesters, vinyl esters, phenolics and epoxies. The microspheres help to significantly increase the stiffness of the finished product without adding a considerable amount of material.

One of its main advantages is the excellent ability to impregnate with a low amount of resin, on average 600 g/m^2 for a thickness of 1 mm. Another key aspect is its adaptability to various application techniques, such as hand lay-up and spray application, which makes it suitable for the manufacture of complex shaped parts or for large volume production [27], [28].

Figure 3. Coremat XI 3 mm [27] [28]

The press mold was layed up with an extraction wax (CIREX CP 10, produced by Airétec, and supplied by RomPolimer Composites, Bucharest, Romania) [29] used for epoxy resins. It has no affinity for the resin or the composite. Each layer of fabric was placed in the press mold, manual laying-up operation was used for resin impregnation into each fabric sheet. The mat was also impregnated with the epoxy resin, by laying-up operation. Then, the composite was pressed at 0.5-0.7 MPa. After maintaining the composite for 8 hours under this pressure, it was demolded, naturally aged for 7 days, at room temperature. After that, a cure treatment at 60°C, for 6 hours, was applied in an oven.

Figure 4 synthetically presents the laboratory technology and the materials for producing the composites, but also, auxiliary equipment and safety personal equipment.

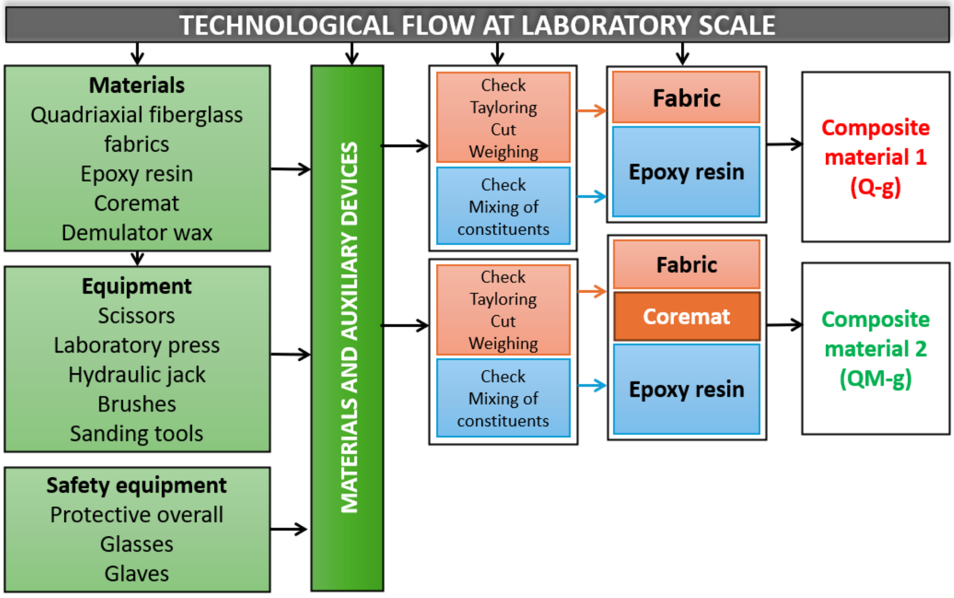

Figure 4. Technological flow at laboratory scale for manufacturing the composite panels

Table 2. Characteristic of the composite plates (300 mm x 300 m) used to cut impact samples

Composite	Plate	Fabric mass, m_f (g)	Total plate mass (g)	Resin mass (g)	Mass fiber ratio	Surface density (kg/m^2)	$V_f/V_{composite}$	$h_{average}$ (mm)
Q-g	1	855.00	1254.5	399.5	0.68	13.93	0.44	8.36
	2	844.50	1351.5	507	0.62	15.01	0.42	8.62
	3	846.50	1300	453.5	0.65	14.44	0.42	8.63
	Average	**848.67**	**1302.00**	**453.33**	**0.65**	**14.47**	**0.43**	**8.54**
QM-g	1	831.00	1361	521.50	0.61	15.12	0.33	10.98
	2	858.00	1362.5	497.50	0.63	15.13	0.34	10.97
	3	860.00	1353	485.00	0.64	15.03	0.34	11.075
	Average	**849.67**	**1358.83**	**501.33**	**0.63**	**15.10**	**0.33**	**11.01**

Table 2 presents the obtained characteristics of composite plates of 300 mm x 300 mm. Fabric mass is the mass of 8 layers, cut from the fabric roller. The small variation of fabric mass reflects the high quality of the quadriaxial fabric.

Several research studies reported the influence of fiber volume fraction (or fiber mass fraction) on mechanical properties of glass fiber composites [30], [31]. The influence of fiber volume fraction was reported by Qiao Y. et al. [32] for a larger range (5% to 50%), but only for tensile tests with low test rate (0.2 mm/min). We calculated this feature of the designed composites (Table 2), for each composite plate of 300 mm x 300 mm, in order to evaluate the change in fiber volume fraction when adding the middle layer of Coremat® Xi 3.

Total plate mass is measured after finishing the edges. Resin mass is the quantity of resin calculated with the relation (1) for the composite Q-g and with relation (2) for composite QM-g

$$m_{resin}=m_{composite}-m_{fabric} \quad (1)$$

$$m_{resin}=m_{composite}-m_{fabric}-m_{mat} \quad (2)$$

where m_{mat} is the mass of Coremat Xi3 taking into account the density given in its datasheet [28]; thus, m_{mat}~8 g for each layer of 300 mm x 300 mm

Aria of composite plate is considered $A_{composite} \sim 0.09\ m^2$

Mass fiber ratio M_f is calculates as

$$M_f = m_{fabric}/m_{composite} \qquad (3)$$

Surface density, ρ_A is calculated with the relation

$$\rho_A = m_{composite}/A_{composite}\ [kg/m^2] \qquad (4)$$

The fiber volume fraction is calculated as

$$V_f = (V_{composite}\ \rho_{composite} - m_{resin})/\rho_f \qquad (5)$$

for composites without mat and

$$V_{fM} = (V_{composite}\ \rho_{composite} - m_{resin} - m_{mat})/\rho_f \qquad (6)$$

for composites with mat.

In the relations (5) and (6), the terms have the following explanations: $V_{composite}$ is the volume of the composite plate, calculated as

$$V_{composite} = l^2\ h_{average} \qquad (7)$$

where l is the size of the square plate (considering l=300 mm) and $h_{average}$ is the average height of the composite plate.

The fiber density is taken as ρ_f=2,540 kg/m^3 for glass fibers. The fiber volume ratio is calculated as

$$R(V_f) = V_f/V_{composite} \qquad (8)$$

for the composite without mat

$$R(V_{fM}) = V_{fM}/V_{composite} \qquad (9)$$

for the composite with mat.

Initial composite plates, as extracted from the press, have dimensions of 300 mm x 300 mm. After finishing the plate edges, small samples of 90 mm x 90 mm, were cut from these plates.

2.2 Test Methodology

Test campaign was established after analysing references [33]-[38]. The range of impact energy for test on glass fiber composites are quite large, from 5 J to 250 J when using drop-test equipment. For this test campaign, we selected three values of impact energy (50 J, 100 J and 150 J) and the drop weight and height were tuned for having the same impact velocity with small tolerances (4.37±0.5 m/s)

Tests were carried out on the drop-test machine Instron CEAST 9350 (Norwood, MA, USA) [39] (from INCAS Bucharest, Romania), with a hemispherical impactor of ϕ16 mm, made of hardened steel (60-62 HRC).

The standard ISO 6603-2:2023 [40], describes a test method for both thermoplastic and thermosetting molding and extrusion materials, but also for composites with ”unidirectional or multi-directional reinforcements such as mats, woven fabrics, woven rovings, chopped strands, combination and hybrid reinforcements, rovings, milled fibers, and sheets made from pre-impregnated materials (prepregs)”, meaning it could be useful for ranking this type of epoxy glass fiber composites, too.

a) b)

Figure 5. The drop-test machine: a) the up-part with the impactor device, b) the down-system including the sample fixing device

The experimental plan included five tests for each composite and impact energy value. The repeatability has good quality, as it could be evaluated from the figures in the Annex. (Figures 10 to 13).

3. RESULTS AND DISCUSSION

Figure 6 presents the tested samples for the extreme values of the impact energy. At the lowest tested impact energy, the print in the composite face is small for both composites, but for the impact energy of 150 J, this print is larger and deeper.

A qualitative difference between the two composite is difficult to be done on these photos, thus, we will analyse the aspect of the parameters' evolution during the impact and we propose a set of numerical parameters extracted from the recorded data from Instron machine.

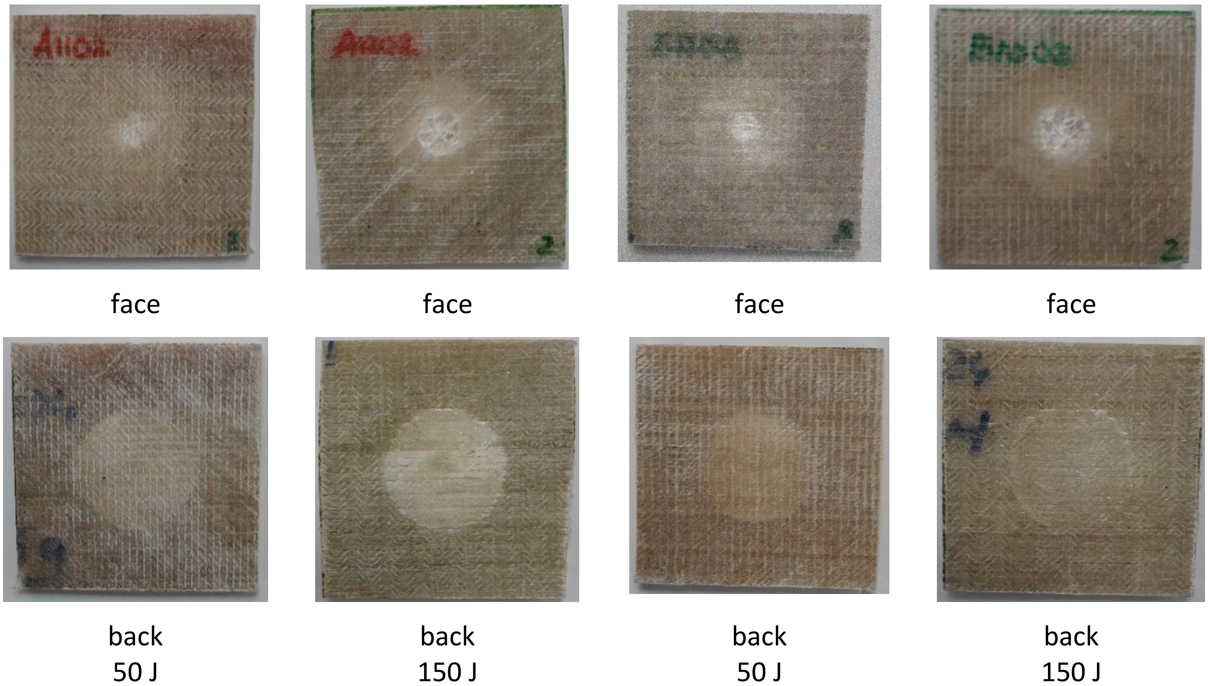

a) Q-g   b) QM-g

Figure 6. Photos of impacted samples for: a) composite Q-g, b) composite QM-g

Figure 7 presents typical curves of the tested samples, meaning curves on middle position from the five ones obtained for each composite and each impact level:

Force – time curves (Fig. 7a) have serrated zones, but the serrations are more pronounced for the composite QM-g (with mat); for the composite without mat, Q-g, the shape is bell-like, and the maximum value increases with the impact energy, from approx. 1600 N at 50 J to approx. 3000 N for an impact energy of 150 J. This characteristic is relevant in marine applications, where composites are frequently subjected to impacts of varying intensity, such as collisions with floating objects, ice or in rough sailing conditions.

The impact duration is also increasing from approx. 4 ms to 6 ms; for the composite without mat; for QM-g, the duration is 4 ms at 50 J, but longer for 100 J and 150 J (6 ms and 8 ms, respectively, and the maximum force remains lower for 100 J and 150 J; only for 50 J the value of is close to that of composite Q-g. This suggests that the mat layer does not significantly influence the behavior of the composite at low impact energy, but clearly makes its presence felt at higher energies.

Examination of force – time curves reveal the significant effect of impact energy on the two materials. For both composites, the maximum force increases with the impact energy; however, the behavior is different. For the QM-g composite, at the maximum energy level (150 J), the curve exhibits a distinct plateau, with lower values than those for Q-g, which means a more stable and longer energy absorption phase. In contrast, for the mat-free composite (Q-g), the force peaks more steeply without a flat area, indicating a stiffer response.

Absorbed energy – time curves (Fig. 7b) have similar shape but the difference between nominal impact energy and the absorbed one is a little bit greater for the composite without mat, meaning the composite QM-g has a larger value for the elastic component of the energy due to the mat. The curves show a gradual ascent until a maximum value of absorbed energy is reached (very very close to the total energy received by the sample during impact).

Displacement – time curve (Fig. 7c) is similar for the impact energy of 50 J, but for 100 J and 150 J, the is higher for the composite QM-g. It is observed that, for all three levels of impact energy, the QM-g composite exhibits higher values of maximum displacement compared to the composite Q-g. This suggests a more pronounced elasticity, i.e. a higher deformation capacity without immediate rupture.

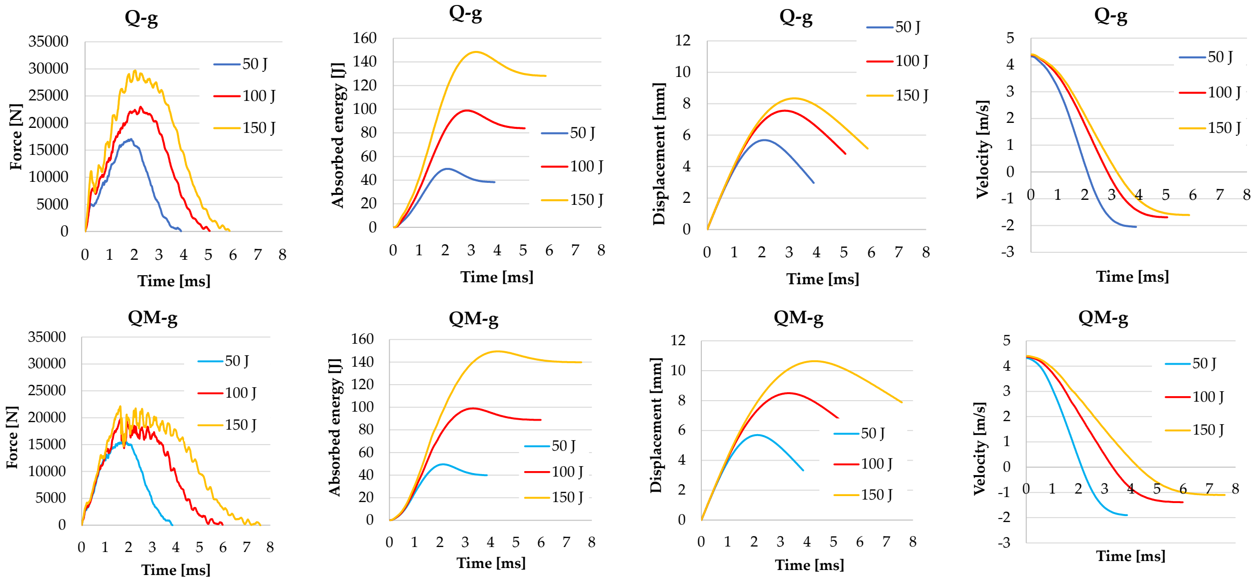

a) b) c) d)

Figure 7. Evolution in time of the fallowing characteristics: a) force, b) absorbed energy, c) displacement, d) velocity

The maximum displacement of composite QM-g denotes a more elastic and adaptive response to impact. The mat layer contributes to additional energy absorption through progressive deformation and retarding the onset of rupture. Therefore, QM-g exhibits a more complex mechanical response, but also more effective impact protection. This progressive deformation capability is extremely valuable in shipbuilding, especially in impact-prone areas such as keel, bow or anchor contact areas.

Velocity – time curves (Fig. 7d) show slopes depending on impact energy, but for the composite Q-g, the difference is small for the impact energies of 100 J and 150 J. The variation of velocity with time is an essential indicator in evaluating the behavior of composites on impact. Immediately after rebound of the impactor, the velocity curves abruptly decrease, reflecting the rapid change in impactor deceleration. For lower values of impact energy (50J), this deceleration is more pronounced, indicating a stiffer material response. As the impact energy increases, the curves indicate a more gradual dissipation of energy. Of particular importance is the point at which the velocity becomes zero, indicating the impactor stop, followed by its rebound (negative velocities). For an energy of 150 J, the Q-g composite (without mat) stops the impactor earlier (~4 ms), while the QM-g stops it later (~6 ms). Although, apparently, Q-g seems more efficient in stopping the impactor, this faster stopping is associated with a higher mechanical shock and damage risk. In contrast, for the composite QM-g, the impact process is slower, signalling safer behavior in applications where gradual energy dissipation is essential. In marine applications, this type of energy dissipation helps to reduce the risk of crack propagation or damage of ship structure, a safer behavior under accidental conditions.

Figures 8 and 9 present average values and standard deviations for 5 tests, for parameters of interest. The data allows for evaluating numerical parameters as the maximum force (F_{max}) (Fig. 8a), the duration till reaching Fmax, coded t(F_{max}) (Fig. 8b), the displacement at F_{max} (d(F_{max})) (Fig. 8c), the absorbed energy at the end of impact (Fig. 9a), impact duration, noted t(F_f=0) (Fig. 9b), and d_{max}.(Fig. 9c).

Even if the impact energy is the same, the maximum force, F_{max}, has lower value for the composite QM-g. If one compares the values for F_{max} taking into account the values for Q-g, F_{max} is lower with 4.44% for impact energy of 50 J, but at 100 J, F_{max} is lower with 17.75%. For the impact energy of 150 J, F_{max} obtained for composite QM-g is with 25.64%.

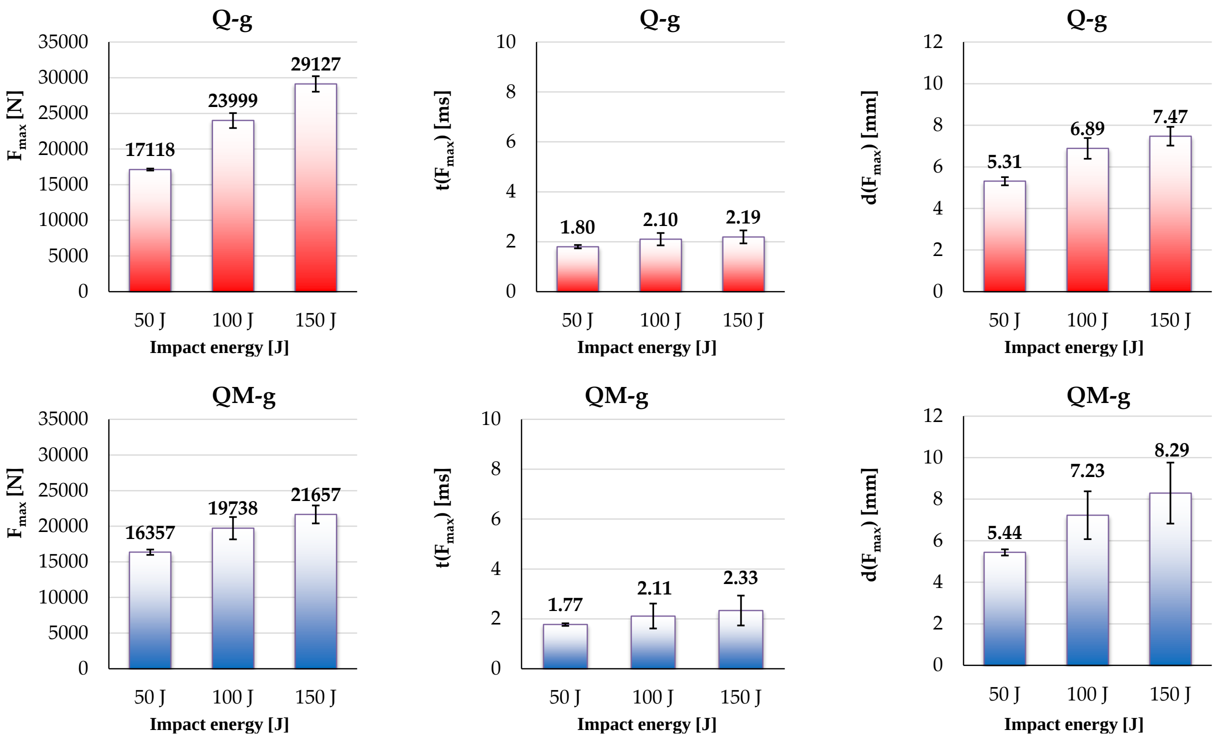

a) b) c)

Figure 8. Characteristics of the tested composites: a) F_{max}, b) time till F_{max}, t(F_{max}), c) displacement till F_{max}, d(F_{max})

Time till F_{max}, t(Fmax) is not so sensitive to material and impact energy (Fig. 8b).

The measured displacement at F_{max}, d(F_{max}), has a similar evolution for both composites, but, as expected, the composite with mat, QM-g, has greater values d(F_{max}) (Fig. 8c), for impact energy of 100 J and 150 J and this is due to mat elasticity and deformation under impactor compression. This difference emphasizes the ability of the mat composite to allow greater deformation without compromising structural integrity, which may be advantageous in applications where controlled deformation is preferable to rapid failure.

For both materials, the values of the maximum force increase proportional to the impact energy. The composite material without mat (Q-g) has higher maximum force values at all three energy levels compared to the composite material with mat (QM-g). For example, at 150 J, Q-g achieves a maximum force of more than 29 000 N, compared to about 21 600 N for QM-g.

This difference can be attributed to the internal structure of the two materials: in the absence of the mat layer, Q-g exhibits a higher stiffness, leading to a higher point mechanical strength, but with a lower energy absorption potential. In contrast, the presence of mat in the QM-g composite leads to more efficient stress distribution and more progressive deformation, which reduces the value of the maximum strength, but may provide more effective protection at the structural scale.

At impact of 50 J, the composite Q-g absorbs 76.84% of the impact energy, at 100 J, 82,82% and at the highest value of tested impact energy, 150 J, this percentage is 85.74%. The composite with mat, QM-g, absorbs 79.66% at 50 J, 89.10% at 100 J and 92.42% at 150 J. Taking this parameter for ranking the composites, the composite with mat has a better behavior. Impact duration is longer for the composite with mat (Fig. 9b), only for impact with 100 J and 150 J. The higher energy absorption indicates a higher potential for dissipation of kinetic energy following impact, which may prevent damage from propagating to adjacent areas of the damaged structure.

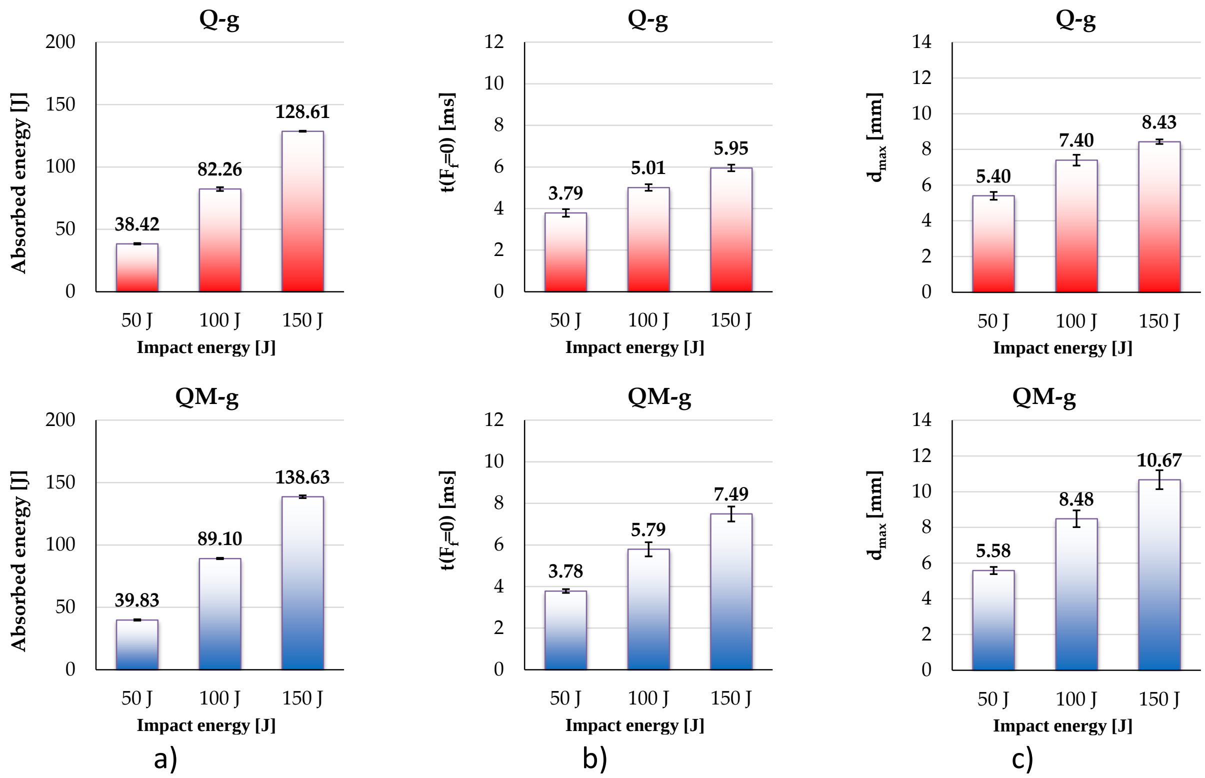

Figure 9. Characteristics of the tested composites: a) absorbed energy, b) impact duration, $t(F_f=0)$, c) maximum displacement, d_{max}

This is particularly relevant in the maritime domain, where structures are exposed to dynamic impacts, and efficient energy dissipation helps to maintain the integrity of the ship under extreme conditions.

Impact duration, $t(F_f=0)$ (Fig. 9b) reflects the total duration of interaction between impactor and hit composite. For composite Q-g, this time gradually increases with the impact energy, from about 3.79 ms at 50 J to 5.95 ms at 150 J. Composite QM-g shows slightly higher values than Q-g, suggesting a longer duration of the absorption energy process, from 3.78 ms at 50 J (insignificat difference from the Q-g composite), to 7.49 ms for 150 J. This prolonged energy absorption of composite QM-g is characteristic of a more elastic and less abrupt response, in which energy is gradually dissipated by internal mechanisms of the material. From an application point of view, a longer interaction time means better energy distribution, reducing the risk of crack propagation. Taking into account that these durations have the order of milliseconds, this is not so relevant for selecting one or another composite.

The maximum displacement, d_{max}, clearly increases with impact energy for both materials, but the values are consistently higher for QM-g. At 150 J, for example, Q-g reaches a maximum displacement of 8.43 mm, while QM-g reaches 10.67 mm (Fig. 9c).

This emphasizes a superior deformation capacity of the composite with, which allows for energy absorption through plastic deformation and internal micro-cracking mechanisms, without total penetration. thus, QM-g exhibits a more elastic and safer behavior in high intensity impacts. this property is extremely useful in naval applications, especially in hull areas or structures frequently subjected to impacts (e.g. in harbors, keels or fenders areas), where controlled deformation can replace sudden damage.

4. CONCLUSIONS

Low-velocity impact tests help select an adequate composite from a class, especially for marine applications.

The maximum force values recorded during impact increase with increasing impact energy for both designed composites (Q-g and QM-g). However, the composite without mat (Q-g) exhibits higher maximum force values, indicating higher stiffness and more aggressive mechanical response, but less capability for dissipating energy progressively.

The composite with mat (QM-g) shows a better controlled deformation capacity, with higher values of maximum displacement and displacement at maximum force. This behavior is associated with a higher elasticity, which allows a more efficient and distributed absorption of impact energy, reducing the risk of sudden cracking.

The maximum force and the total interaction time with the impactor increase with increasing impact energy. The parameter values for QM-g are marginally increased, which means a higher elastic response and more progressive shock absorption - essential attributes for materials used in protective construction.

The energy absorbed by the two materials increases in proportion to the impact energy, but the composite with (QM-g) exhibits slightly higher values, especially at highest tested impact energy (150 J). This difference, although modest in quantitative terms, is significant in functional terms, indicating a higher efficiency in dissipating mechanical energy.

Examination of the velocity-time curves reveals a more regulated response of the QM-g composite, which reduces the velocity of the impactor over a longer period of time, with a gentler slope, indicating a more gradual energy transfer. In contrast, the Q-g composite produces a faster and more pronounced rebound, indicating steeper absorption and higher stiffness.

The impact behavior of the QM-g composite is defined by increased deformation, moderately increased energy absorption, and extended duration of interaction with the impactor, making it suitable for applications that prioritize structural safety and regulated energy dissipation.

The obtained results are relevant to the maritime sector, where materials are often exposed to dynamic loads and the ability to absorb and dissipate energy efficiently is essential for maintaining the structural integrity of the ship.

QM-g composite material, characterized by enhanced elasticity and balanced performance, offers significant benefits in key areas of shipbuilding, including keel, bow and protective compartments.

ACKNOWLEDGEMENT

The authors express their gratitude to National Institute for Aero-space Research "Elie Carafoli" (INCAS), Bucharest, for support in experimental work.

ORCID iDs

Ioana Gabriela CHIRACU 0009-0003-4934-9545
Constantin GEORGESCU 0000-0003-4503-5576
George Cătălin CRISTEA 0000-0002-9190-1327
George Ghiocel OJOC 0000-0002-5666-6659
Mihail BOȚAN 0000-0002-2036-3509
Alexandru Viorel VASILIU 0009-0006-1028-9161
Lorena DELEANU 0000-0001-9161-163X

REFERENCES

[1] C. Long (ed.), ”Design and manufacture of textile composites”, *Elsevier*, 2005.

[2] K. K. Chawla, ”Composite materials: science and engineering”, *Springer Science & Business Media*, 2012.

[3] M. Singha and K. Singha, ”Applications of Textiles in Marine Products”, *Marine Science*, 2012, 2(6): 110-119, DOI: 10.5923/j.ms.20120206.01.

[4] J. Summerscales, ”Materials selection for marine composites”, in ”Marine Composites, J. Pemberton, J. Summerscales and J. Graham-Jones, (eds.), *Woodhead Publishing, Elsevier*, Duxford, United Kingdom, 2019; pp. 3-30.

[5] J.R Weitzenböck, B. Hayman, G. Hersvik, D. McGeorge, P. Noury, D. M. Hill and A. Echtermeyer, ”Application of Composites. In Proceedings Ships and Offshore – A Review and Outlook”, *Marine and Offshore Composites*, The Royal Institution of Naval Architects, RINA HQ, London, United Kingdom, 3–4 February 2010.

[6] J.Graham-Jones and J. Summerscales, ”Introduction, Part Two Applications of Advanced Fibre-Reinforced Composites”, in ”Marine Structures Marine Applications of Advanced Fibre-Reinforced Composites; J. Graham-Jones and J. Summerscales (eds.), *Woodhead Publishing, Elsevier*, Cambridge, United Kingdom, 2016; pp. 1-24.

[7] F. Rubino, A. Nisticò, F. Tucci and P. Carlone, ”Marine application of fiber reinforced composites: A review”, *Journal of Marine Science and Engineering*, 2020, 8(1), 26. https://doi.org/10.3390/jmse8010026.

[8] A. Wahrhaftig, H. Ribeiro and A, Nogueira, ”A structural composite for marine boat constructions”, in ”Marine Composites. Design and Performance”, R. Pemberton, J. Summerscales and J. Graham-Jones (eds.), *Woodhead Publishing, Elsevier*, Duxford, United Kingdom, 2019, pp. 301-314.

[9] S. Patil, D. M. Reddy and M. Reddy, ”Low velocity impact analysis on composite structures–A review”, First International Conference on Design, Materials and Manufacture (ICDEM 2018), 1943 (1), 020009. *AIP Publishing LLC*; Karnataka, India, 29–31 January 2018. https://doi.org/10.1063/1.5029585], the failure mechanisms.

[10] S. Zhang, ”The Mechanics of Ship Collision”, PhD thesis, Technical University of Denmark, Lyngby, Denmark, 1999.

[11] K. Yang, S. Wu, J. Guan, Z. Shao and R. O. Ritchie, ”Enhancing the Mechanical Toughness of Epoxy-Resin Composites Using Natural Silk Reinforcements”, *Scientific Reports*, 2017, 7, 11939, DOI:10.1038/s41598-017-11919-1

[12] A. P. Mouritz, E. Gellert, P. Burchill and K. Challis, ”Review of advanced composite structures for naval ships and submarines”, *Composite Structures*, 2001, 53, pp. 21–42, https://doi.org/10.1016/ S0263-8223(00)00175-6

[13] A. Caramatescu and C. I. Mocanu, ”Review of composite materials applications in marine industry”, *The Annals of “Dunarea de Jos” University of Galati, Fascicle XI – Shipbuilding*, 2019, pp. 169-174.

[14] P. Davies, ”Evaluation of New Composite Materials for Marine Applications”, *Applied Composite Materials*, 2024, 31, pp 1933-1954, https://doi.org/10.1007/s10443-024-10232-1.

[15] Z. Zhu, X. Li, Q. Chen, Y. Cai and Y. Xiong, ”Simulations and Tests of Composite Marine Structures Under Low-Velocity Impact”, *Polish Maritime Research*, 2021, 281 (109); pp. 59-71, 10.2478/Pomr-2021-0006

[16] Y.-J.; Jeong, H.-T.; Kim, J.-D.; Kim, J.-H.; Kim, S.-K.; Kim and J.-M Lee, ”Evaluation of mechanical properties of glass fiber-reinforced composites depending on length and structural anisotropy”, *Results in Engineering*, 2023, 17,

101000, https://doi.org/10.1016/j.rineng.2023.101000.
[17] C. Bouvet and S. Rivallant, ”Damage tolerance of composite structures under low-velocity impact. In Dynamic Deformation, Damage and Fracture”, in ”Composite Materials and Structures”, 2nd ed., V. Silberschmidt (ed.), *Woodhead Publishing, Elsevier Ltd*. Cambridge, USA, 2022; pp. 3-28, https://doi.org/10.1016/B978-0-12-823979-7.00002-8.
[18] G. Maloy Smith ”Impact Testing Explained: Methods, Applications, and Benefits”, 2024, https://dewesoft.com/blog/impact-testing-explained (accessed 11.12.2024).
[19] L. S. Sutherland and C. Guedes Soares, ”Impact on Marine Laminates. In Proceedings of the RINA Conference on the Modern Yacht”, Southampton, United Kingdom, 11-12 October 2007, DOI: 10.13140/RG.2.1.4559.1760.
[20] 1200 g/m2 Quadriaxial Stitched Glass Fabric (0º/+45º/90º/-45º), 127 cm wide https://www.castrocompositesshop.com/en/fibre-reinforcements/1204-1200-gm2-quadriaxial-stitched-glass-fabric-0%C2%BA45%C2%BA90%C2%BA-45%C2%BA-127-cm-wide.html (accessed 10.01.2022).
[21] L. S. Sutherland, R. A. Shenoi and S. M. Lewis, ”Size and scale effects in composites: II. Unidirectional laminates”, *Composite Science Technology*, 1999, DOI: 10.1016/S0266-3538(98)00083-9.
[22] G. G. Ojoc, ”A Theoretical and Experimental Study of Ballistic Protection Packages Made of Glass Fibers”, PhD Thesis, “Dunarea de Jos” University, Galati, Romania, 2022.
[23] Ultimare Glassfiber and Resin Guidebook, https://fiberglasswarehouse.com/blogs/news/ultimate-fiberglass-and-resin-guidebook-for-beginners (accessed 10.09.2024).
[24] C. Jubsilp, P. Mora, C. W. Bielawski, Z. Lu, And S. Rimdusit, ”13 - Thermosetting matrix based glass and carbon fiber composites”, in ”Fiber Reinforced Composites, Compatibility, Perspectives and Applications”, Joseph K., Oksman K., George G., Wilson R., Appukuttan S., Eds.; *Woodhead Publishing*, Cambridge, United Kingdom; 2021, pp. 341-403, https://doi.org/10.1016/B978-0-12-821090-1.00012-0.
[25] Advanced Composites Solutions. High Performance Epoxy and Polyurethane Systems file:///D:/Downloads/advanced-compositessolutions.pdf (accessed 4.10.2024).
[26] SikaBiresin® CR82 (formely Biresin® CR82), https://industry.sika.com/en/home/advanced-resins/sports-and-leisure/composite-resin-systems/composite-systemsforwetlay-up/sikabiresin-cr82.html (accessed 5.04.2024).
[27] Lantor 3mm Xi Coremat (50mts) https://grpukltd.com/product/lantor-3mm-xi-coremat-50mts/ (accessed 3.12.2024).
[28] Composites. Datasheet Coremat® Xi, https://grpukltd.com/wp-content/uploads/2016/10/Xi.pdf (accessed 8.12.2024).
[29] Demulanti / Agenti de lustruire, https://www.rompolimer.ro/produse/demulanti-agenti-lustruire/ (accessed 9.11.2024).
[30] C. Larco, R. Pahonie and I. Edu, ”The Effects of Fibre Volume Fraction on a Glass-Epoxy Composite Material”, *INCAS Bulletin*, 7/3/ 2015, pp. 113–119, DOI: 10.13111/2066-8201.2015.7.3.10.
[31] S. Asmare, B. Yoseph, and T. M. Jamir, ”Investigating the impact resistance of E-glass/ Polyester composite materials in variable fiber-to-matrix weight ratio composition”, *Cogent Engineering*, 2023, 10(1). https://doi.org/10.1080/23311916.2023.2178110
[32] Y. Qiao, S. Ko, J. L. Ramos, E. K. Nickerson, A. C. Denny, G. M. Schuler, N. L. Brown, A. Guzman, C. E. Moriel, M. R. Pallaka, Y. Ni, K. W. Shahwan and K. L. Simmons, ”Effects of processing temperature, pressure, and fiber volume fraction on mechanical and morphological behaviors of fully-recyclable uni-directional thermoplastic polymer-fiber-reinforced polymers”, *Composites. Part C*, 2024, 14, 100497, https://doi.org/10.1016/j.jcomc.2024.100497
[33] L. A. Carlsson, D. F. Adams and R. B. Pipes, ”Experimental characterization of advanced composite materials”, *CRC Press*, Boca Raton, USA; 2014.
[34] A. Vescovini, J. A. Cruz, D. Ma, C. Colombo, A. Salerno, O. Bianchi, S. C. Amico, and A. Manes, ”Experimental investigation on low-velocity impact behavior of glass, Kevlar and hybrid composites with an elastomeric polyurethane matrix”, *Compososites Part C*, 2024, 13, 100426, https://doi.org/10.1016/j.jcomc.2023.100426.
[35] A. S. AlOmari, K. S. Al-Athel, Arif, A.F.M.; and F. A. Al-Sulaiman, ”Experimental and Computational Analysis of Low-Velocity Impact on Carbon-, Glass- and Mixed-Fiber Composite

Plates", *Journal of Composites Science,* 2020, 4, 148. https://doi.org/10.3390/jcs4040148.

[36] R. Olsson and S. Sicomp, "Low- and medium-velocity impact as a cause of failure in polymer matrix composites", in "Failure mechanisms in polymer matrix composites", P. Robinson, E. Greenhalgh and S. Pinho (eds.), *Woodhead Publishing Limited*, Cambridge, United Kingdom, 2012; pp. 53-78.

[37] I. Păduraru, G. G. Ojoc, H. Petrescu, I. Graur, C. Pîrvu and L. Deleanu, "The Behavior of Glass Fiber Composites under Low Velocity Impacts", *Polymers*, 2023, 15, 4549. https://doi.org/10.3390/polym15234549.

[38] T. S.Reddy, P. R.Subba Reddy and V. Madhu, V., "Low velocity impact studies of E-glass/epoxy composite laminates at different thicknesses and temperatures", *Defence Technology*, 2019, 15/6, pp. 897-904, https://doi.org/10.1016/j.dt.2019.02.003.

[39] CEAST 9300 Series. Droptower Impact Systems, WB1268C, 2009, Illinois Tool Works Inc., SUA, https://www.instron.com/-/media/literature-library/products/2010/02/ceast-9300-series.pdf (accessed 9.10.2024).

[40] ISO 6603-2:2023 Plastics. Determination of puncture impact behaviour of rigid plastics — Part 2: Instrumented impact testing.

Annex

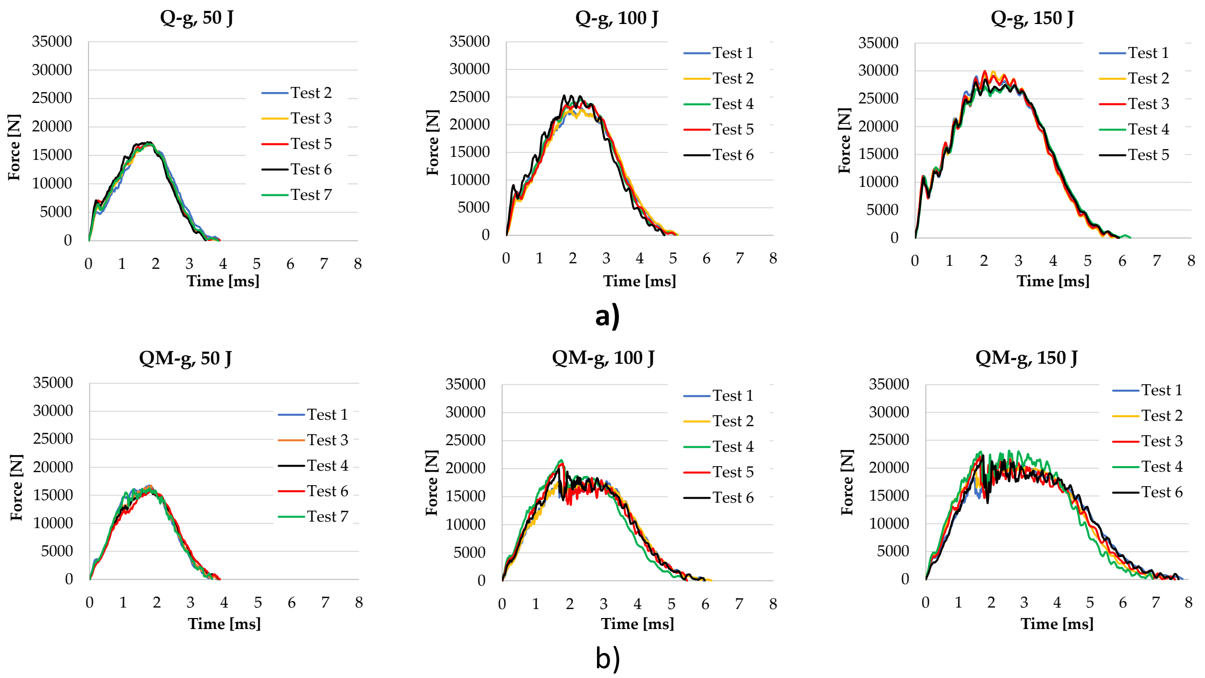

Figure 10. Curves force – time for a) composite Q-g, b) composite QM-g

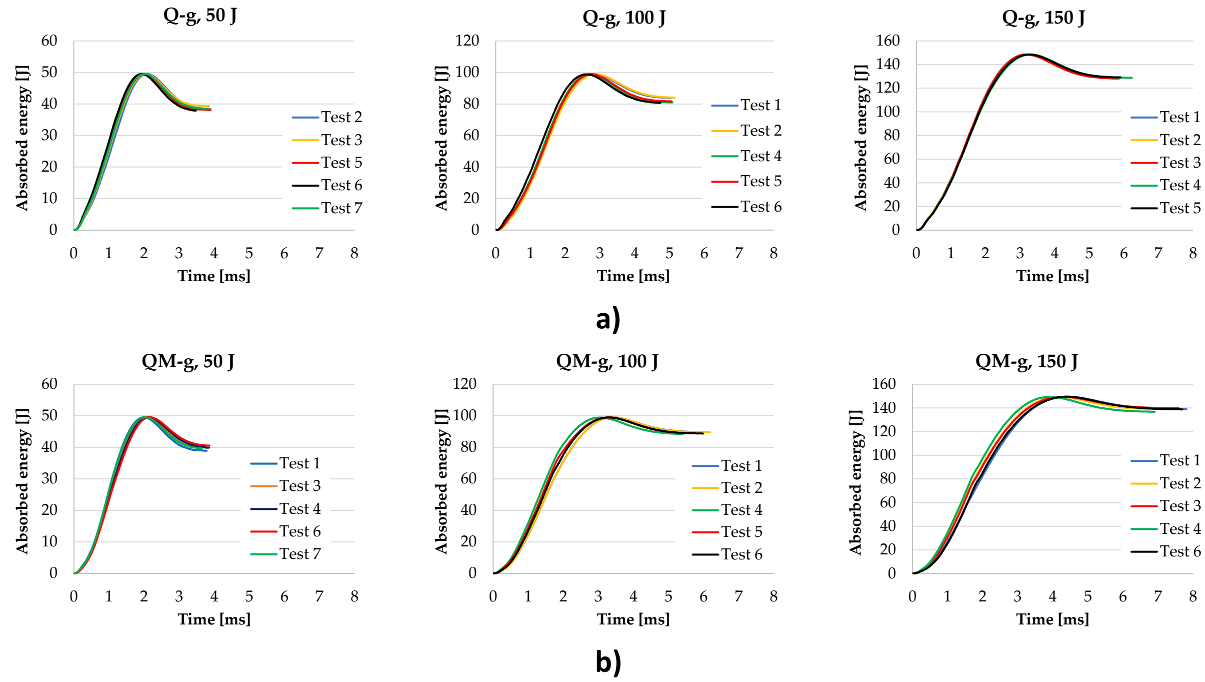

Figure 11. Curves absorbed energy – time for a) composite Q-g, b) composite QM-g

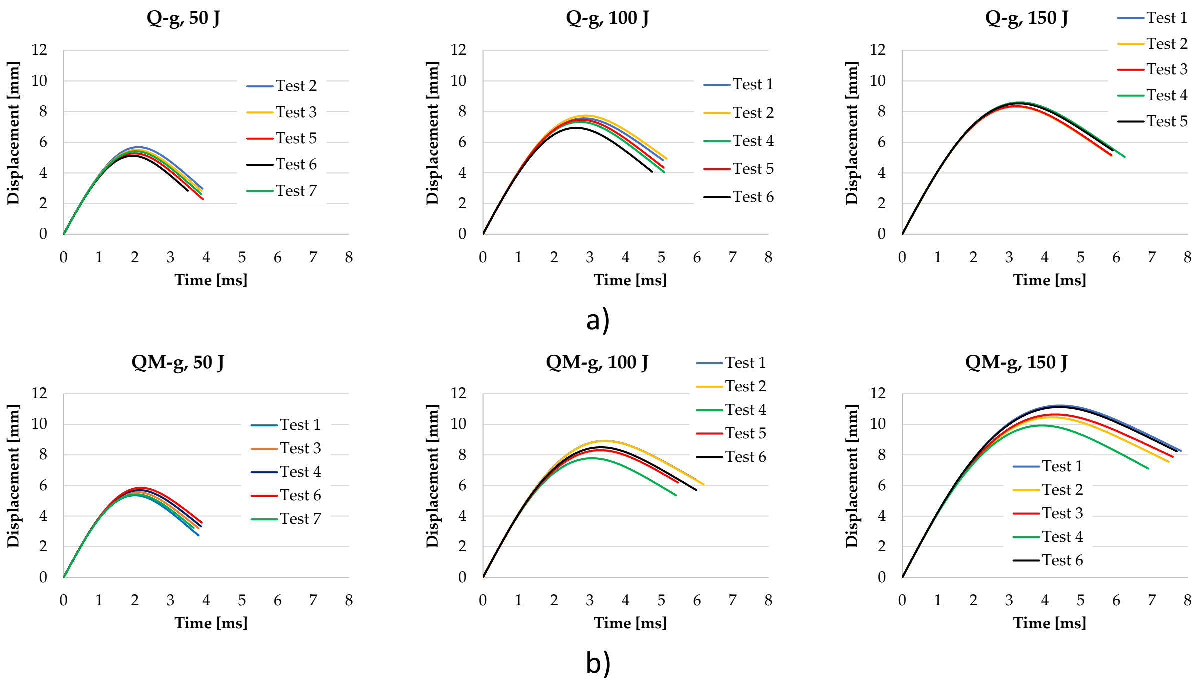

Figure 12. Curves displacement – time for a) composite Q-g, b) composite QM-g

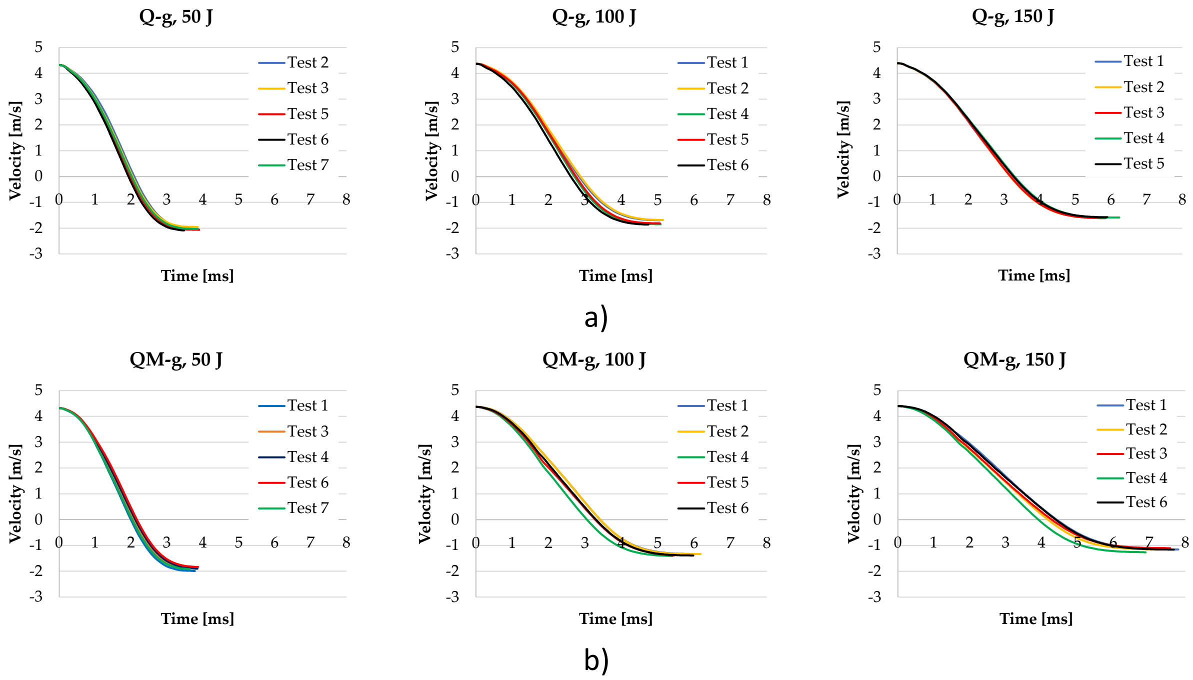

Figure 13. Curves velocity – time for a) composite Q-g, b) composite QM-g